SIMULATION TOOLS AND APPLICATIONS

IMACS EUROPEAN SIMULATION MEETING

Győr, Hungary
28-30 August 1995

PROCEEDINGS

Edited by András JÁVOR

NUMERICAL SIMULATION OF FLUID FLOWS IN A DIFFERENTIALLY HEATED ROTATING ANNULUS

B G Sherlock,
Department of Electrical Engineering, Parks College of Saint Louis University, 500 Falling Springs Road, Cahokia, Illinois, 62206, USA.

Q G Rayer,
Nuclear Electric Plc., Berkeley Technology Centre, Berkeley, Gloucestershire, GL13 9PB, UK.

S Ahmed,
Department of Computer Science, Parks College of Saint Louis University, 500 Falling Springs Road, Cahokia, Illinois, 62206, USA.

ABSTRACT

Three dimensional unsteady incompressible fluid flow in a uniformly rotating frame is solved using a new approach. The governing equations of fluid motion are discretized using a control-volume procedure, ensuring that global conservation laws are obeyed. Pressure and velocities are calculated iteratively at each time-level, yielding a semi-implicit scheme. Buoyancy effects are included by using the Boussinesq approximation. The form of the energy equation neglects the presence of internal energy point sources and sinks, viscous dissipation of energy and work done by the body force, though it would be simple to incorporate these effects into the scheme if desired. The model will be tested by using it to simulate the three dimensional incompressible flow in a fluid annulus rotating with uniform angular velocity. Differential heating is provided by maintaining the side-walls of the convection chamber at separate temperatures.

INTRODUCTION

The study of rotating differentially heated fluids can contribute to the understanding of geophysical systems such as the atmosphere and oceans [1]. The differentially heated rotating fluid annulus (see Figure 1) represents such systems in an idealised form, allowing basic fluid processes to be elucidated, as well as being a fluid dynamical system of considerable interest in its own right. The simple, well defined boundary conditions of the annular convection chamber make it a suitable model for numerical investigation.

The present paper reports the formulation of a new computer model of the annulus based on the control-volume scheme [2,3]. Previous computer models of the rotating fluid annulus have used grid-point finite-difference formulations which only conserve mass, momentum and energy in the limit as the simulation mesh becomes infinitely fine. They have been applied not only to unobstructed flows [4-6], but also to flows where the annulus was fully blocked by a thermally insulating radial barrier [7,8]. The finite-difference model has so far failed to simulate several aspects of the flow in a annulus blocked by a radial barrier. Rayer [7] noticed defects in the velocity fields that may be similar to those mentioned by White [6]. Also this model did not calculate the correct value for the temperature drop observed across the thermally insulating barrier during experimental work. This may be due to an absence of sufficient grid points adjacent to the barrier to represent the boundary layer that may be present there.

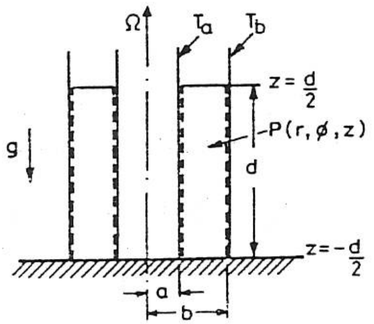

Fig. 1. Diagram of fluid annulus. (r,ϕ,z) are cylindrical polar coordinates of a general point P, fixed in a frame moving with the annulus which rotates uniformly at Ω rad.sec^{-1}. The upper surface is in contact with a rigid lid [9]. $\Delta T \equiv T_b - T_a = 4$ or 10 °C, a=2.5cm, b=8.0cm, d=14.0cm.

To address these problems a new annulus code has been constructed using the control-volume scheme of approach [3]. The details of this new formulation follow.

THE COMPUTER MODEL

The new model uses the control-volume approach [3]. The discretization equation obtained by this method expresses the global conservation principles for quantities such as mass, momentum and energy so that they are exactly conserved over the calculation domain. By expressing the parameters of the problem in non-dimensional terms it is possible to use the Boussinesq approximation for three-dimensional incompressible flow in a uniformly rotating frame. The reference velocity and characteristic time for the non-dimensionalization are

$$|\Omega|L=\omega L, \text{ and } \frac{1}{|\Omega|}=\frac{1}{\omega},$$

where $|\Omega|=\omega$ and L is a characteristic length scale. Then the non-dimensional variables become

$$x^*=\frac{x}{L},\ u^*=\frac{U}{\omega L},\ t^*=\omega t,\ \mu^*=\frac{\mu}{\mu_0},\ \rho^*=\frac{\rho}{\rho_0},\ k^*=\frac{k}{k_0},\ T^*=\frac{T-T_0}{T_b-T_0}$$

$$\text{and } p^*=\frac{p-\rho_0 g(d-z)-\frac{1}{2}\rho_0\omega^2 r^2}{\rho_0\omega^2 L^2}.$$

Where the parameters listed above are; position vector, $\underline{x}=(r,\phi,z)$; fluid velocity, $\underline{u}^*=(u^*,v^*,w^*)$; reference fluid velocity $\underline{U}=(U,V,W)$; time, t; fluid viscosity, μ; fluid density, ρ; thermal conductivity, k; temperature, T; mean fluid temperature, T_0; pressure, p and gravity, g. With these definitions the operators become,

$$\frac{\partial}{\partial t}=\omega\frac{\partial}{\partial t^*},\text{ and }\nabla=\frac{1}{L}\nabla^*,\text{ where }\nabla^*=\hat{x}_i\frac{\partial}{\partial x_i^*}.$$

Thus using the Boussinesq approximation, the conservation equations for three-dimensional incompressible baroclinic flow in a rotating frame can be written in non-dimensional form as

$$\frac{\partial \underline{u}^*}{\partial t^*}+\nabla^*.(\underline{u}^*\underline{u}^*)=-\nabla^*p^*+\mathrm{Gr}(\mathrm{Ro}^2)T^*\hat{z}-r^*\alpha^*T^*\hat{r}-2u^*\hat{\phi}+2v^*\hat{r}+\mathrm{Ro}\nabla^{*2}\underline{u}^*, \quad (1)$$

where the Grashoff number, Gr and Rossby number, Ro, are

$$\mathrm{Gr}=\frac{\rho_0^2 g L^3\alpha(T_b-T_0)}{\mu_0^2},\text{ where }\alpha^*=\alpha(T_b-T_0),\text{ and }\mathrm{Ro}=\frac{\mu_0}{\rho_0\omega L^2}.$$

α is the coefficient of thermal expansion, and T_b the temperature of the hot side-wall. The energy equation becomes

$$\frac{\partial T^*}{\partial t^*}+(\underline{u}^*.\nabla^*)T^*=\frac{\mathrm{Ro}}{\mathrm{Pr}}\nabla^*.(k^*\nabla^*T^*),$$

where Pr is the Prandtl number,

$$\mathrm{Pr}=\frac{\mu_0 C_{P0}}{k_0}.$$

Equation (1) can be differenced in a control-volume manner with respect to the staggered grid and control-volume shown in Figure 2 to yield the discretized conservation law in Box 1. The fluxes at the cell faces are calculated by the upwind approximation at each face. Discretization equations for the other flow variables were obtained in a similar manner. The numerical scheme proceeds by calculating u, v and w at the n+1 time-level explicitly from the Navier-Stokes momentum equations. In general, this solution will not satisfy the continuity equation. Following the approach of Patankar [2] a Poisson equation for a pressure correction is solved,

$$\nabla^2 p'=-\frac{1}{A}\nabla.\underline{u},$$

where A is a fictitious time interval, followed by a velocity correction

$$\underline{u}'=A\nabla p'.$$

The corrected velocities and pressures are used to construct the fluxes at the cell faces. Upon iteration, this process yields the velocities at the n+1 time-level which satisfy both the momentum and continuity equations. Because of the iterative update of the fluxes, the scheme is semi-implicit. The energy equation is then solved for the fluid temperature at time-level n+1 in an explicit manner, using the newly calculated velocity field. Marching in time is continued

$$
\begin{aligned}
&\frac{u^{n+1}_{i+\frac{1}{2}}-u^{n}_{i+\frac{1}{2}}}{\Delta t}+\frac{\left[u_{i+1}u_{i+1}r_{i+1}-u_i u_i r_i\right]}{r_{i+\frac{1}{2}}\Delta r_{i+\frac{1}{2}}}+\frac{1}{r_{i+\frac{1}{2}}\Delta\phi_j}\Big[(uv)_{i+\frac{1}{2},j+\frac{1}{2}}\cos(\phi_{j+\frac{1}{2}}-\phi_j)- \\
&(uv)_{i+\frac{1}{2},j-\frac{1}{2}}\cos(\phi_j-\phi_{j-\frac{1}{2}})-v^2_{i+\frac{1}{2},j+\frac{1}{2}}\sin(\phi_{j+\frac{1}{2}}-\phi_j)-v^2_{i+\frac{1}{2},j-\frac{1}{2}}\sin(\phi_j-\phi_{j-\frac{1}{2}})\Big] \\
&+\frac{1}{\Delta z_k}\Big[(uw)_{i+\frac{1}{2},k+\frac{1}{2}}-(uw)_{i+\frac{1}{2},k-\frac{1}{2}}\Big]= \\
&\mathrm{Ro}\Bigg\{\frac{(u_{i+\frac{3}{2}}-u_{i+\frac{1}{2}})r_{i+1}}{\bar{r}\Delta r_{i+\frac{1}{2}}\Delta r_{i+1}}-\frac{(u_{i+\frac{1}{2}}-u_{i-\frac{1}{2}})r_i}{\bar{r}\Delta r_{i+\frac{1}{2}}\Delta r_i}+\frac{u_{i+\frac{1}{2},j+1}\cos(\phi_{j+1}-\phi_j)-u_{i+\frac{1}{2}}}{\bar{r}r_{i+\frac{1}{2}}\Delta\phi_j\Delta\phi_{j+\frac{1}{2}}} \\
&\frac{u_{i+\frac{1}{2}}-u_{i+\frac{1}{2},j-1}\cos(\phi_j-\phi_{j-1})}{\bar{r}r_{i+\frac{1}{2}}\Delta\phi_j\Delta\phi_{j-\frac{1}{2}}}-\frac{u_{i+\frac{1}{2},j+1}\sin(\phi_{j+1}-\phi_j)}{\bar{r}r_{i+\frac{1}{2}}\Delta\phi_j\Delta\phi_{j+\frac{1}{2}}} \\
&+\frac{u_{i+\frac{1}{2},j-1}\sin(\phi_j-\phi_{j-1})}{\bar{r}r_{i+\frac{1}{2}}\Delta\phi_j\Delta\phi_{j-\frac{1}{2}}}+\frac{u_{i+\frac{1}{2},k+1}-u_{i+\frac{1}{2}}}{\Delta z_k\Delta z_{k+\frac{1}{2}}}-\frac{u_{i+\frac{1}{2},k}-u_{i+\frac{1}{2},k-1}}{\Delta z_k\Delta z_{k-\frac{1}{2}}}\Bigg\}.
\end{aligned}
$$

Box 1. Discretized conservation law.

until the changes in the flow variables are sufficiently small to indicate the procedure has converged.

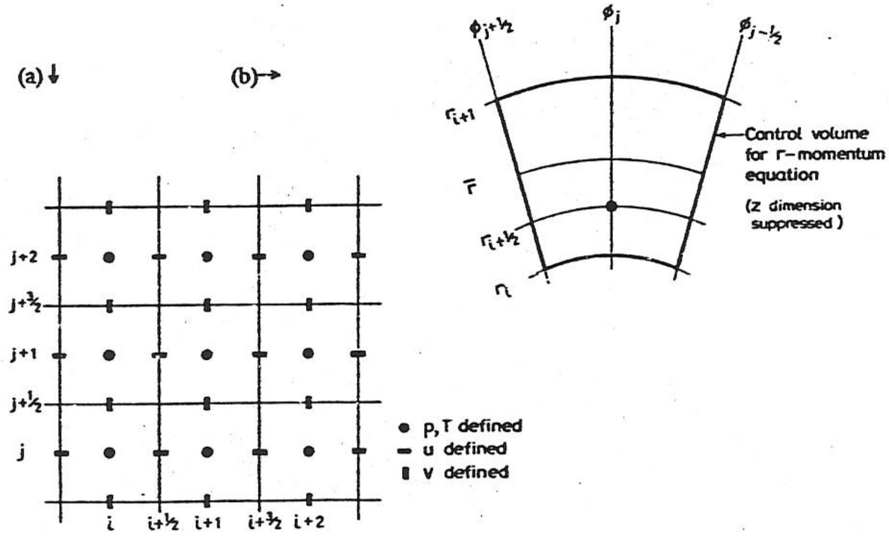

Fig. 2. (a) Staggered grid used in control-volume formulation. (b) Typical control-volume in (r,ϕ) plane.

MODEL RESULTS

Some typical flows calculated by the model for a temperature difference of 4°C and a rotation rate of 0.5 rad.sec^{-1} are given in Figure 3. The plots are in the form of fluid velocity vectors plotted in the (r,z) plane opposite the barrier (Figure 3a) and in the (r,ϕ) plane at mid-depth in the fluid (Figure 3b). Figure 3(a) shows fluid rising by the hot outer cylinder at r=8.0cm, and sinking by the cold inner cylinder at r=2.5cm, accompanied by radial inflow near the top of the convection chamber and radial outflow at the bottom. This aspect of the simulated flow is consistent with experimental observations, though the circulations in a horizontal plane (Figure 3b) differ somewhat from Rayer [7]. The results also show that vertical velocities are inhibited in the body of the fluid, as would be expected by consideration of the Taylor-Proudman theorem [10], so that vertical motions take place mainly in the side-wall boundary-layers.

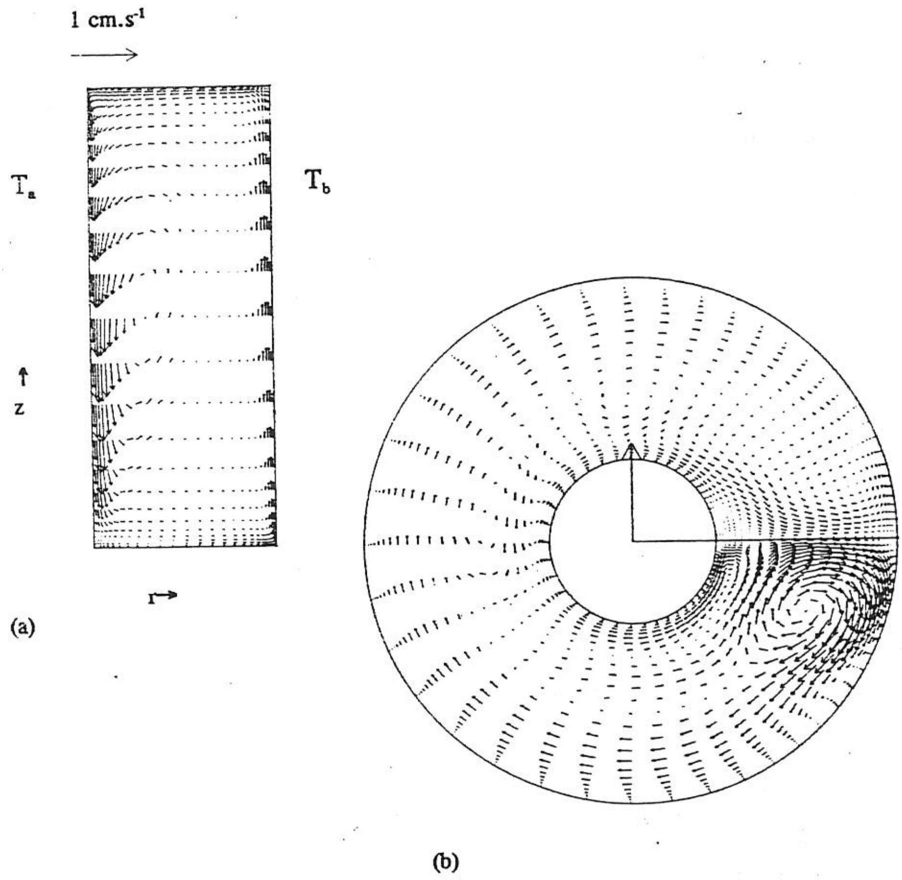

Fig. 3. Fluid velocity vector plots, $\Delta T=4°C$, $\Omega=0.5$ rad.sec^{-1}, the scale arrow denotes a velocity of 1 cm.s^{-1}. (a) Flow in the (r,z) plane opposite the radial barrier. (b) Flow in the (r,ϕ) plane at mid-depth in the annular convection chamber.

REFERENCES

1 R Hide (1977), Experiments with rotating fluids, Quart J Roy Met Soc, 103, 1-28.

2 S V Patankar (1980), Numerical heat transfer and fluid flow, Hemisphere, ISBN 0-89116-919-9.

3 D A Anderson, J C Tannehill and R H Pletcher (1984), Computational fluid mechanics and heat transfer, Hemisphere Pub Corp, New York, ISBN 0-89116-471-5.

4 I N James, P R Jonas and L Farnell (1981), A combined laboratory and numerical study of fully developed steady baroclinic waves in a cylindrical annulus, Quart J Roy Met Soc, 107, 51-78.

5 P Hignett, A A White, R D Carter, W N D Jackson, and R M Small (1985), A comparison of laboratory measurements and numerical simulations of baroclinic wave flows in a rotating cylindrical annulus, Quart J Roy Met Soc, 111, 131-154.

6 A A White (1988), The dynamics of rotating fluids: numerical modelling of annulus flows, Met Mag, 117, 54-63.

7 Q G Rayer (1992), An experimental investigation of heat transfer by large-scale motions in rotating fluids, D Phil thesis, Oxford University, UK.

8 Q G Rayer (1994), A numerical investigation of the flow in a fully blocked differentially heated rotating fluid annulus, Int J Modern Phys C, Vol 5, No 2, 203-206.

9 W W Fowlis and R Hide (1965), Thermal convection in a rotating annulus of liquid: effect of viscosity on the transition between axisymmetric and non-axisymmetric flow regimes, J Atmos Sci, 22, 541-558.

10 J Proudman (1916), On the motion of solids in a liquid possessing vorticity, Proc Roy Soc London A, 92, 408-424.